

Relationship Between the Extent of Chromosomal Losses and the Pattern of CpG Methylation in Gastric Carcinomas

The extent of unilateral chromosomal losses and the presence of microsatellite instability (MSI) have been classified into high-risk (high- and baseline-level loss) and low-risk (low-level loss and MSI) stem-line genotypes in gastric carcinomas. A unilateral genome-dosage reduction might stimulate compensation mechanism, which maintains the genomic dosage via CpG hypomethylation. A total of 120 tumor sites from 40 gastric carcinomas were examined by chromosomal loss analysis using 40 microsatellite markers on 8 chromosomes and methylation analysis in the 13 CpG (island/non-island) regions near the 10 genes using the bisulfite-modified DNAs. The high-level-loss tumor (four or more losses) showed a tendency toward unmethylation in the *Maspin*, *CAGE*, *MAGE-A2* and *RABGEF1* genes, and the other microsatellite-genotype (three or fewer losses and MSI) toward methylation in the *p16*, *hMLH1*, *RASSF1A*, and *Cyclin D2* genes ($p < 0.05$). The non-island CpGs of the *p16* and *hMLH1* genes were hypomethylated in the high-level-loss and hypermethylated in the non-high-level-loss sites ($p < 0.05$). Consequently, hypomethylation changes were related to a high-level loss, whereas the hypermethylation changes were accompanied by a baseline-level loss, a low-level loss, or a MSI. This indicates that hypomethylation compensates the chromosomal losses in the process of tumor progression.

Key Words : Chromosomal Loss; Aneuploidy; CpG Methylation; DNA Methylation; Dosage Compensation (Genetics); Stomach Neoplasms; Prognostic Genotype; Genetic Phenomena

Seung-Jin Hong, Young-Ho Kim,
Young-Deok Choi, Ki-Ouk Min*,
Sang-Wook Choi¹, Mun-Gan Rhyu

Departments of Microbiology, Clinical Pathology* and
Internal Medicine¹, College of Medicine, The Catholic
University of Korea, Seoul, Korea

Received : 3 March 2005
Accepted : 21 April 2005

Address for correspondence

Mun-Gan Rhyu, M.D.
Department of Microbiology, College of Medicine
The Catholic University of Korea, 505 Banpo-dong,
Socho-gu, Seoul 137-701, Korea
Tel : +82-2-590-1220, Fax : +82-2-596-8969
E-mail : rhyumung@catholic.ac.kr

*This study was supported by a grant from Korea
Science and Engineering Foundation; Grant number
'R01-1999-000-00108-0'.

INTRODUCTION

A genetic instability is believed to underlie the various genomic changes in a malignancy (1). In solid tumors, unilateral chromosomal losses are the most common genetic events that are detected as a loss of heterozygosity (LOH) using highly polymorphic microsatellite markers (2). The extent of the unilateral chromosomal losses and the microsatellite instability (MSI) detected in stage II and III gastrointestinal carcinomas (3, 4) have been classified into high-level LOH (LOH-H) and baseline-level LOH (LOH-B) in those with a poor prognosis and low-level LOH (LOH-L) and MSI in those with a low risk. Gastric carcinomas frequently display an intratumoral heterogeneity with the different histological types and varying degrees of differentiation (5, 6). Previous multifocal LOH studies on gastric carcinomas (7, 8) reported the extent of the chromosomal losses as a stem-line genotype commonly shared by heterogeneous tumor sites. This suggests that the level of chromosomal losses plays a master role in the diverse progression of gastric carcinomas.

Chromosomal losses detected by LOH analysis, in a naive sense, represent an imbalanced loss or a dose reduction of the genetic elements. A difference in the dose of the X chromo-

some between males (XY) and females (XX) is equalized via a dosage compensation mechanism, which randomly inactivates one of two X chromosomes via DNA hypermethylation (9). The X-to-autosomal chromosome ratio is believed to inherently initiate the methylation changes in order to maintain the genomic dosage in mammals (10, 11). Although solid tumors suffer from global DNA hypomethylation and multiple gene-specific hypermethylation (12), the link between the unilateral chromosomal losses and DNA methylation is poorly understood in terms of the genetic and epigenetic interaction including the compensative methylation changes in response to a genome dosage reduction. Therefore, it is important to determine if the extent of the chromosomal losses is related to the pattern of DNA methylation changes.

Hypomethylation and hypermethylation involve the different spectra of cancers in distinct fashions. The genomic and gene-specific hypomethylation closely correlate with advanced-stage cancers (13, 14). Meanwhile, gene-specific hypermethylations are widely detected in different subsets of gastrointestinal cancers with and without MSI (15, 16). At the genomic level, global hypomethylation of the cancer genome is only an insignificant change affecting a small por-

tion of the non-coding genetic elements in the gene- and GC-poor heterochromatin region (14, 17). However, GC-rich regions adjacent to the coding genes frequently exhibit hypermethylation in the undermethylated CpG islands (15) and hypomethylation in the overmethylated non-island CpGs (13), suggesting a methylation variation that is prone to hyper- and hypomethylation changes in cancer cells. Therefore, it is likely that both hypermethylation and hypomethylation, each of which plays a distinct role in diverse tumor progression, can be detected in the methylation variation regions adjacent to the genes.

In this study, multifocal analysis on gastric carcinomas was carried out to determine the relationship between the stem-line extent of the chromosomal losses and the CpG methylation status in heterogeneous tumor tissues. A total of 120 tumor foci from 40 gastric carcinomas were examined to determine the extent of chromosomal losses using a PCR-based LOH analysis on 8 cancer-associated chromosomal arms. The 13 extragenic regions adjacent to the 10 cancer-related or -unrelated genes were evaluated for the methylation status of the CpG islands and/or the non-island CpGs using methylation-specific PCR (MSP) and bisulfite sequencing analyses. The proportion of methylation and unmethylation was compared to determine the rise and fall in the methylation density in the paired normal and tumor tissues.

MATERIALS AND METHODS

Patients and tumor tissues

The gastric carcinoma tissues were selected from those that had been recently resected in a similar period because formalin-fixed paraffin-embedded tissue DNA tends to be poorly amplified by PCR in the older archives. Fifty patients who were suspected of having a gastric carcinoma were underwent a surgical resection at the St. Paul's Hospital, The Catholic University of Korea between March and December 2002. Of the 50 patients, 40 patients, who were suitable for isolating the matching normal and tumor DNAs from the paraffin-embedded tissues, and for providing the clinicopathological information, were enrolled in this study. The normal lymph nodes were also collected as the control. The nontumoral gastric mucosa was examined for the presence or absence of intestinal metaplasia. The histological type of the gastric carcinoma was classified into intestinal, diffuse, and mixed according to the Lauren classification (18) and the degree of differentiation was graded according to the WHO classification. The clinicopathological tumor stage was determined using the Tumor-Node-Metastasis (TNM) criteria (19). Permission for this study was obtained from the Institutional Review Board and written informed consent was obtained from each patient prior to the surgical resection.

Three tumor sites per gastric carcinoma were selected from

the topographically opposite and histologically distinct areas. A tissue area ranging from 5 mm to 7 mm in diameter was microdissected from an average of 10 consecutive seven- μ m-thick hematoxylin-eosin-stained sections using a stereomicroscope under a $\times 40$ magnification. All the microdissected tumor sites were checked for the tumor cell contents $\geq 70\%$ prior to DNA extraction. A tumor cell content of 80-89% held a major fraction (74 sites, 62%) of the microdissected tissue sites followed by $\geq 90\%$ (29 sites, 24%) and 70-79% (17 sites, 14%) of the tumor cell contents. Approximately 50 microdissected cells were digested in 1 μ L of a Tween 20-Proteinase K lysis buffer. An average of 100 μ L of the tissue lysate from each microdissected site was examined for its LOH status, and an average of 500 μ L of the lysate was subjected to bisulfite modification to determine the methylation status (Fig. 1). Because the digested tissue admixture contained genomic DNA of heterogeneous quality in different concentration, the amount of template DNA used for the PCR-based microsatellite and methylation analyses was determined based on the PCR band intensity of 20 ng/ μ L amplified by a microsatellite primer set, *D19S226* (forward, 5'-CCA GCA GAT TTT GGT GTT GTC TA-3'; reverse, 5'-ACA GAG CCA GAG CCA GTA GGA GT-3'; amplicon size, 164 bp).

Microsatellite analysis

PCR amplification of the template DNA was performed under the so-called "multiplex, hot-start" condition using a radioisotope (α - 32 P dCTP, PerkinElmer, Boston, MA, U.S.A.) as described previously (7, 8). For each PCR, two pairs of microsatellite primers were used, and the template-primer mixtures were heated prior to adding the dNTP and *Taq* DNA polymerase (Takara, Shiga, Japan). One μ L of the template DNA was amplified and labeled through 32 PCR cycles using a thermocycler (iCycler, Bio-Rad, Hercules, CA, U.S.A.) as follows: 1 min of denaturation at 94°C, 1 min of annealing at 58-64°C, and 1 min of elongation at 72°C in a 10 μ L reaction mixture. Of the PCR products, 5 μ L was loaded directly onto a sequencing gel containing 7 M urea and visualized by repeated autoradiography using a radioluminograph scanner (BAS 2500, Fuji Photo Film, Kanakawa, Japan). The optimal range of the band intensities was measured by densitometry using TINA image software (Raytest Isotopenme β gerate GmbH, Straubenhardt, Germany). Each reaction was repeated twice and the same band intensity was confirmed.

The MSI and LOH status were defined using a panel of 40 microsatellite markers that were selected from eight chromosomes, including 3p, 4p, 5q, 8p, 9p, 13q, 17p, and 18q, as described previously (Fig. 1A) (7, 8). The MSI status of the microsatellite sequences was scored if frameshift mutations were observed in $>40\%$ of the homozygous markers. Because increased instability in the repeated sequences obscured the LOH status in most microsatellite markers, a LOH was scored in those cases without a MSI. A reduction in the allelic inten-

sity in the tumor tissue was scored as a LOH if the normalized ratio of the heterozygous alleles had decreased to the cut-off point of less than 0.65-fold intensity reduction.

The lost extent of a chromosomal arm was determined based on the number of allelic losses, and was classified into either a constitutional loss involving more than one microsatellite allele or an interstitial loss involving only one allele. The extent of the chromosomal losses in each case was scored according to the number of constitutional chromosomal losses causing a significant reduction in the genomic dosage. According to the classification criterion for the extent of the chromosomal losses reported previously (7, 8), the intestinal-type gastric carcinomas were divided into low-level (LOH-L, three or fewer losses) and high-level (LOH-H, four or more losses) loss groups, and the diffuse-type carcinomas were divided into the baseline-level (LOH-B, zero or one loss), low-level (LOH-L, two or three losses), and high-level (LOH-H, four or more losses) loss groups.

DNA modification by sodium bisulfite

Ninety microliters of the tissue lysate were denatured with

10 μ L of 3 M NaOH for 15 min at 37°C. The mixture was then modified with 1,040 μ L of 2.3 M sodium bisulfite and 60 μ L of 10 mM hydroquinone for 12 hr at 50°C, and purified using the Wizard DNA purification resin (Promega, Madison, WI, U.S.A.) according to the manufacturer's instructions (20). The modified DNA was finally precipitated by adding 2.5 volumes of 100% ethanol and 1 μ L of salmon testis DNA (5 mg/mL, Sigma-Aldrich, St. Louis, MO, U.S.A.). The pellet was washed with 70% ethanol, dried, and dissolved in 35 μ L of a 5 mM Tris buffer (pH 8.0). In order to avoid repeated freezing and thawing, a 1 μ L aliquot of the modified DNA solution was placed in a PCR tube and stored at -20°C.

The genomic DNA universally methylated by DNA methylase (CpGenome Universal Methylated DNA, Chemicon, Temecula, CA, U.S.A.) was used as the methylation control DNA. The PCR DNA that had been amplified by a universal primer (5'-CCG ACT CGA GNN NNN NAT GTG G-3') was used as the unmethylation control DNA. Universal PCR was carried out as follows: 1 cycle of denaturation at 94°C for 3 min, 10 cycles of 94°C for 1.5 min, 30°C for 2.5 min, a ramp at 0.1°C/sec to 72°C, 72°C for 3 min and 30 cycles of 94°C for 1 min, 62°C for 1.5 min, 72°C for 2 min, and 8

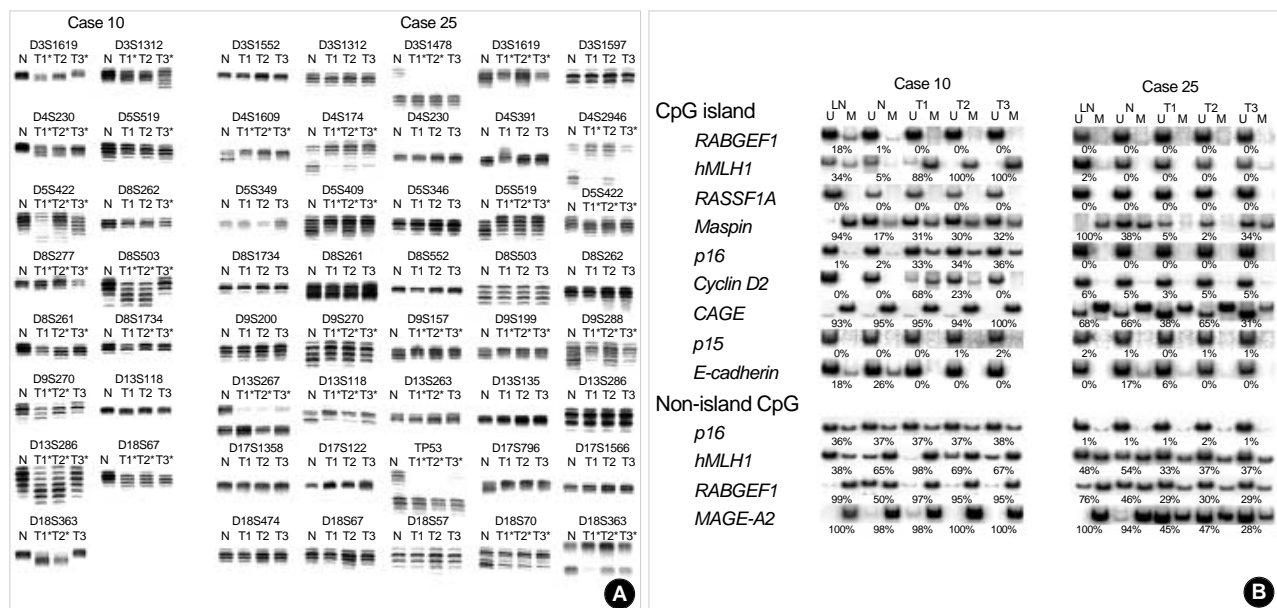


Fig. 1. Representative autoradiographs of the multifocal microsatellite and methylation analyses. (A) Case 10 shows a high-frequency microsatellite instability (MSI) at more than 40% of the 15 homozygous markers in the three tumor sites (T1, 67%; T2, 73%; T3, 80%). Case 25 had a high-level loss of heterozygosity (LOH) involving chromosomes 3p, 4p, 5q, 9p, 13q, 17p, and 18q commonly shared by the three tumor sites. Normal (N) and the corresponding tumor (T) DNAs are indicated above each allelic band. The asterisk indicates a MSI or LOH. (B) Normal lymph node (LN), nontumoral gastric mucosa (N), and multiple tumor sites (T1, T2, and T3) have a broad range of methylated and unmethylated amplification from the bisulfite-modified DNAs. The lanes marked by U and M indicate the PCR bands of the unmethylation and methylation primer sets, respectively. The methylated and unmethylated proportion of the *Maspin* CpG islands and the *RABGEF1* non-island CpGs was obviously different between the normal lymph node and the gastric mucosa of case 10 and 25. Case 10 with a MSI shows diverse increases in the methylated proportion of the CpG islands of the *hMLH1*, *Maspin*, *p16*, and *Cyclin D2* genes as well as the non-island CpGs of the *hMLH1* and *RABGEF1* genes. In case 25 with a high-level chromosomal loss, the unmethylated proportion of the CpG islands of the *Maspin* and *CAGE* genes and the non-island CpGs of the *hMLH1*, *RABGEF1* and *MAGE-A2* genes are increased in a similar or dissimilar grade. The percentage of methylated CpGs in the template DNA calculated based on the standard MSP curve (Fig. 2) is indicated below the lanes. The results of microsatellite and methylation analyses are summarized in Tables 2 and 5, respectively.

min of elongation at 72°C.

Methylation density analysis

Methylation analysis using the radioisotope was performed in minimal of amplification rounds in order to avoid excessive DNA amplification. One μL of the bisulfite-modified DNA was amplified and labeled by a hot-start PCR containing $\alpha\text{-}^{32}\text{P}$ dTTP (PerkinElmer, Boston, MA, U.S.A.) and dNTP mixture through 32 PCR cycles. Bisulfite-modified DNAs produced a total PCR intensity of 2-10 ng/ μL by each MSP primer set. Of the PCR products, 5 μL was loaded directly onto a nondenaturing polyacrylamide gel and visualized by repeated autoradiography using a radioluminograph scanner.

An initial study validated the high specificity of each MSP primer set using the methylation and unmethylation control DNA. The standard curves for the MSP primers were plotted according to the methylation and unmethylation band intensities that were amplified from various mixtures of the

two control DNAs (Fig. 2). The proportion of the methylation and unmethylation band intensities against the total intensity of each MSP primer set showed a linear relationship between the percentage of the methylation and unmethylation control DNAs in the template-primer mixtures. Based on the standard curve of the control MSP bands, the reciprocal proportion of methylation and unmethylation bands (Fig. 1B) was graded as complete unmethylation (0-20% methylation, zero methylation), low density methylation (21-40% methylation, one methylation), moderate density methylation (41-60% methylation, two methylation), high density methylation (61-80% methylation, three methylation), and complete methylation (81-100% methylation, four methylation).

Methylation- and unmethylation-specific PCR and bisulfite sequencing

The MSP primer sets were designed in order to assess the small fragment less than 150 bp, which stably amplified

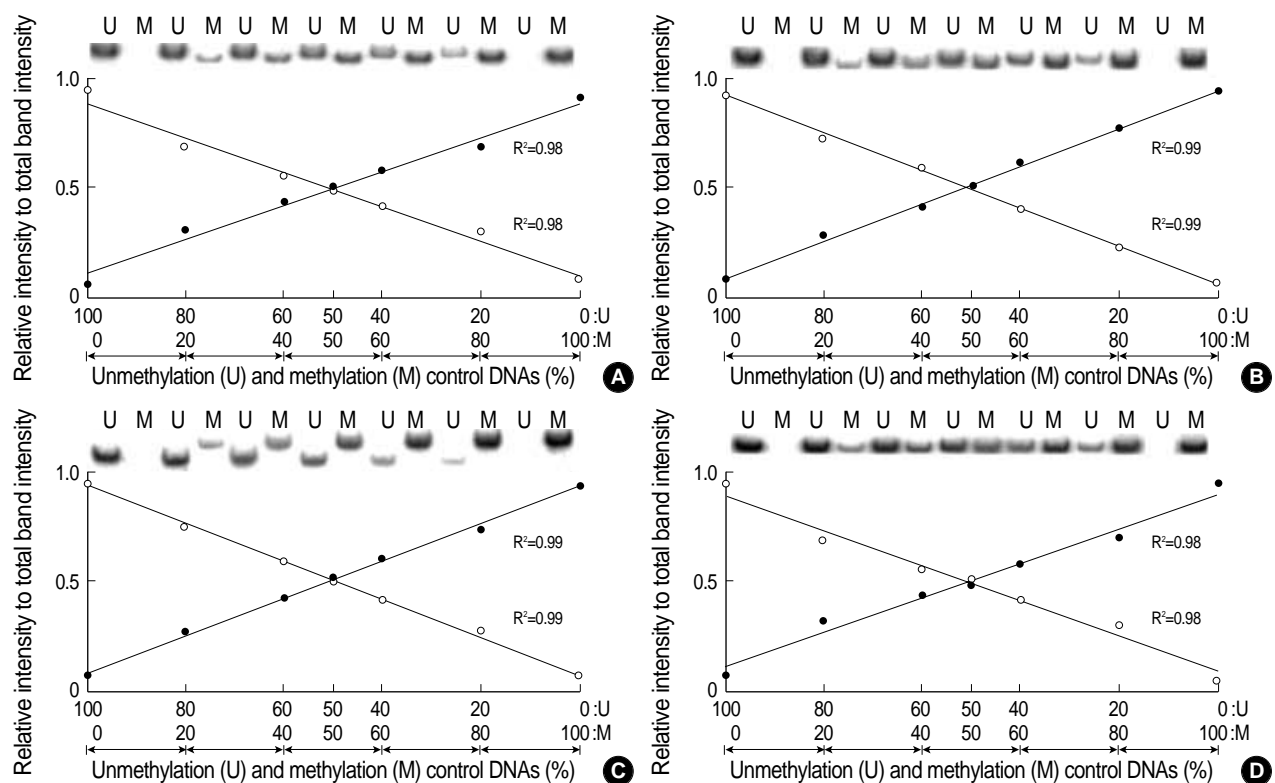


Fig. 2. Standard curves for the methylated and unmethylated MSP amplification. The genomic DNA universally methylated by DNA methylase and the genome-wide-PCR DNA amplified by a universal primer were used as the positive controls for the methylation and unmethylation DNAs, respectively. The variable mixtures of the two opposite control DNAs based on their PCR intensity of 20 ng/ μL were amplified using a set of MSP primers. The band intensities of the methylation (M, closed circle) and unmethylation (U, open circle) primer sets for the CpG islands of the *hMLH1* (A), *Maspin* (B), and *CAGE* (C) genes and the non-island CpGs of *hMLH1* gene (D) are plotted along with the relative proportion against the total band intensity. The amplification intensity ratio of each primer set is linearly increased with the increasing percentage of the corresponding control DNA in the MSP template-primer mixtures. The methylation-unmethylation proportion of the template DNA was distinguished into five grades (0-20% methylation, 21-40% methylation, 41-60% methylation, 61-80% methylation, and 81-100% methylation) based on the reciprocal curves of the methylation and unmethylation bands. The band intensity ratio of each MSP primer set is listed in Table 1.

the template DNAs from the obtained formalin-fixed paraffin-embedded tissues. The primer sequences were selected using a MethPrimer software (<http://www.urogene.org/meth-primer/>), and were checked for any sequence redundancy by BLAST search (<http://www.ncbi.nlm.nih.gov/BLAST/>). Two different CpG regions adjacent to the transcription start site were accessed in this study. The CpG islands at a CpG_{Obs/Exp} ratio >0.6 resided within the extragenic regions 1 kb proximal to the genic regions, whereas the upstream regions more than 1 kb distant from the genes showed a low number of CpG site (Table 1). The MSP primer sets for the CpG islands of the *bMLH1* (21), *RASSF1A* (22), *p15* (23) genes and the non-island CpGs of *MAGE-A2* (24) gene were based on those described elsewhere.

Two or three CpG sites within the MSP primer sequences were found to amplify the specific methylation and unmethylation band intensities from the control DNAs. The non-island CpGs, which had a relatively low CpG content, was insufficient to facilitate the primer design in some cases. These CpG primer sets introduced the non-specific bands to the counterpart control DNAs. Thirteen out of the 17 primer sets tested amplified only a specific band intensity ratio ≥ 0.9 from both the methylation and the unmethylation control DNAs (Table 1). Finally, a panel of 13 MSP primer sets were selected from the upstream regions adjacent to the *p15*, *p16*, *bMLH1*, *E-cadherin*, *RASSF1A*, *MAGE-A2*, *CAGE*, *Maspin*, and *Cyclin D2* genes, in which one or more reports described the hypo- or hypermethylation changes in gastric carcinomas, as well as an arbitrarily selected *RABGEF1* gene.

The methylation composition of each template DNA copy

was analyzed by bisulfite sequencing. The methylation-unmethylation common primer sets encompassing the MSP primer sequences were used. The PCR products common to the methylated and unmethylated CpGs were cloned into the pCR2.1-TOPO vector (Invitrogen, Carlsbad, CA, U.S.A.), and the PCR clones from each genomic DNA were cycle-sequenced using a BigDye Terminator Kit (PE Biosystems, Foster City, CA, U.S.A.) and an ABI automated DNA sequencer (PE Biosystems, Warrington, U.K.).

Statistical analysis

The statistical comparisons of the clinicopathological features between the different microsatellite genotypes were performed using an independent t test and a χ^2 test or Fisher's exact test. Mann-Whitney *U* and Kruskal-Wallis nonparametric tests were used to compare the methylation status according to the level of chromosomal losses and the clinicopathological parameters. Two-sided *p*-values less than 0.05 were considered significant.

RESULTS

Multifocal analysis of microsatellite alterations

Of the 40 gastric carcinomas, three had a high-frequency MSI at more than 40% of the homozygous alleles in multiple tumor sites examined (Fig. 1A, Table 3). A total of 411 chromosomal losses were detected in 111 tumor sites from

Table 1. CpG dinucleotides examined by the methylation-specific polymerase chain reaction

Coding gene	Chromosome locus	CpG _{Obs/Exp}	GC%	5' position*		Intensity ratio [†]		
				U	M	U	U/M	M
CpG island								
<i>RABGEF1</i>	7q11.21	0.95	63.5	-284	-282	0.90	0.46/0.54	0.91
<i>hMLH1</i>	3p22	0.86	68	-664	-669	0.94	0.48/0.52	0.93
<i>RASSF1A</i>	3p21.3	0.81	70	106	118	0.92	0.46/0.54	0.93
<i>Maspin</i>	18q21.43	0.8	45	-314	-309	0.93	0.51/0.49	0.94
<i>p16</i>	9p21	0.79	74.5	-218	-218	0.91	0.47/0.53	0.91
<i>Cyclin D2</i>	12p13.32	0.79	72	-1,229	-1,226	0.92	0.48/0.52	0.93
<i>CAGE</i>	Xq22.11	0.77	55	-63	-92	0.94	0.48/0.52	0.94
<i>p15</i>	9p21	0.74	70	95	99	0.91	0.48/0.52	0.91
<i>E-cadherin</i>	16q22.1	0.62	69.5	-106	-104	0.92	0.49/0.51	0.94
Non-island CpG								
<i>Cyclin D2</i>	12p13.32	0.59	52.5	-2,326	-2,325	0.75	0.58/0.42	0.54
<i>MAGE-A2</i>	Xq28	0.52	66	-389	-386	0.74	0.45/0.55	0.90
<i>p16</i>	9p21	0.48	61.5	-1,581	-1,576	0.90	0.47/0.53	0.93
<i>CAGE</i>	Xq22.11	0.40	50.5	-1,447	-1,447	0.56	0.37/0.63	0.93
<i>hMLH1</i>	3p22	0.38	51.5	-1,107	-1,107	0.93	0.51/0.49	0.95
<i>Maspin</i>	18q21.43	0.38	51	-972	-972	0.56	0.39/0.61	0.78
<i>RABGEF1</i>	7q11.21	0.29	65	-8,630	-8,628	0.91	0.48/0.52	0.90
<i>MAGE-A2</i>	Xq28	0.18	58.5	-1,440	-1,439	0.90	0.54/0.46	0.91

*The genomic positions were calculated from the July 2003 human genome reference sequence. [†]The relative proportion of the unmethylation (U) and methylation (M) primer sets against the total band intensity. The nucleotide sequences and PCR condition of each primer set are provided in the Table 2.

37 MSI-negative cases. Of these, 389 (95%) were counted as being constitutional losses involving more than one microsatellite marker on a chromosomal arm. Thirteen (35%) out of the 37 LOH-positive gastric carcinomas were found to be composed of genetically different subclones in terms of the intratumoral LOH clonality. Six cases had heterogeneous LOHs involving the upper and lower opposite alleles on the same chromosome.

In a comparison of the LOH heterogeneity rate (Table 4), the mixed- and diffuse-type gastric carcinomas (61%), advanced-stage diseases (69%) and the small sized tumors ≤ 5 cm in diameter (69%) showed frequent LOH heterogeneity. However, as a result of the reciprocal losses of the opposite alleles on the same chromosomes, a difference in the genomic dosage reduction between the heterogeneous tumor sites was no greater than one chromosomal loss. In most LOH-positive cases (35 out of 37), the same or a similar number of chromosomal losses detected in heterogeneous tumor sites was classified into the same category of chromosomal losses (Table 3).

Case 28, who contained two (low level) and four (high level) losses, was defined as a LOH-H genotype detected in two of the three tumor sites examined. Case 22 containing no constitutional chromosomal losses was classified into a LOH-B genotype based on the predominance of a diffuse-type histology. Consequently, 4 LOH-B (10%), 16 LOH-L (40%), 17 LOH-H (42.5%), and 3 MSI (7.5%) cases were identified in the 40 surgical specimens examined. In a comparison of the clinicopathological variables between the LOH-H and LOH-L gastric carcinomas (Table 5), a lymphatic invasion ($p=0.005$) and advanced stage ($p=0.002$) were significantly associated with the LOH-H cases.

Methylation status of the nontumoral tissues

A total of 13 CpG regions examined showed various methylation densities in the nontumoral tissues including the gastric mucosa, gastric intestinal metaplasia and lymph nodes, which variably changed in the heterogeneous tumor sites (Fig.

Table 2. Sequences and PCR condition of the methylation-specific PCR primer sets

		Forward (5' to 3')	Reverse (5' to 3')	Size	Tm (°C)	
CpG island	<i>RABGEF1</i>	U	AAGTIGGAAGTAGGGATTGAGI	C AAAATAAAAATACCACCCTAAC A	131	58
		M	GTCCGAAGTAGGGATTGAGC	G AAATAAAAATACCGCCCTAACG	128	58
	<i>hMLH1</i>	U	TTTTGATGTAGATIGTTTTATTAGGGTIGI	ACCACCTCATCA TAACTACCCACA	124	58
		M	ACGTAGACGTTTTATTAGGGTCCG	CCTCATCGTAACTACCCGCG	112	58
	<i>RASSF1A</i>	U	TTGGTTGGAGTGTGTTAAIGIG	CAAACCCCA CAACTAAAAACA A	105	58
		M	GTGTTAACGCGTTGCGTATC	AACCCCGCGAACTAAAAACGA	93	58
	<i>Maspin</i>	U	GAATATTTATTTTTIGGTTTTGIG	AAAAAACCTCCAACATATTCA	111	56
		M	TTATTTTTCGGTTTTGCG	AAAAAACCTCCAACATATTCCG	104	54
	<i>p16</i>	U	TGTTATTTTIGTTTTAGGIG	AAAACCTCAAACCAATCCCA	130	56
		M	TGTTATTTTCTGTTCTGAGGC	AAAACCTCAAACCGTTCCGA	129	58
	<i>Cyclin D2</i>	U	GGAGGTGAAGAAATGTTATTAGATI	TCTCCCTAAAAACCACTACA	140	59
		M	GGTGAAGAAACGTTATTAGATC	TCCCTAAAAACCGACTACG	134	55
	<i>CAGE</i>	U	TGGTTTTGGGGTAATTTTTGI	CAATCTACAACCTATTTCCCA	105	57
		M	TTTTATACGATTCGGAATTCGAC	CAATCTACGACCTATTTCCCG	136	58
	<i>p15</i>	U	TGTGATGIGTTIGTATTTTIGGTT	CCATACAATAACCAAACAACCA	154	58
		M	GCGTTCTGATTTTCTGCGTT	CGTACAATAACCGAACGACCGA	148	58
	<i>E-cadherin</i>	U	GGTGAATTTTAGTTAATTAGTGGTAI	TCACAAATACTTTACAATTCACA	108	56
		M	TGAATTTTTAGTTAATTAGCCGGTAC	ACAAATACTTTACAATTCACGAC	104	58
Non-island CpG	<i>p16</i>	U	TIGGGATTAGGTTTAGTTTTIGG	CTATAAAACCCTATCAACTCACACT	130	58
		M	TCCGGATTAGGTTTAGTTTTCG	AAACCCTATCGACTCACGCT	125	60
	<i>hMLH1</i>	U	GATTTTAGGATTGTIGATATGAGI	AAACTACCTCCTAATCTTTATCCA	126	58
		M	GATTTTAGGATTGTGATATGAGC	AACTACCTCCTAATCTTTATCCG	125	58
	<i>RABGEF1</i>	U	ATTAAGGGTAGTTAGAAIGTTIIGG	AAACCCAAAACCTCACTTATAAACCA	124	58
		M	TAAGGGTAGTTAGAACTGTTCCGG	CCAAAAACTCGCTTATAAACG	119	60
	<i>MAGE-A2</i>	U	GTTAGGTIGTTGTTTAGGGI	CCAAAAAATCACAAACCCA	92	59
		M	GCGTTTGTTTTTTCTGTCGAC	AAATCACGAACCCGAATATAACG	108	61
	Common primer	<i>hMLH1*</i>	GAAGGAGGTTAYGGGTAAG	TAATCTATCRRCCCTCATC	155	60
		<i>hMLH1†</i>	TGTTGTTGTAGGGATTTTAGGATTG	CCTATAAAAACCTACCTCCTAATCT	146	57
		<i>p16*</i>	AATTGTAGATTGGGATTTAYG	CRTACBCAAAACCTCAAACC	169	56
		<i>p16†</i>	CAAACCTCACTTCTCC	GGGTGTGTGTAGAGGATT	197	60
		<i>MAGE-A2</i>	GGGTGAGGTTYGTTTAG	TCCACCCTTACCR TAAACCC	189	57

*CpG island area. †Non-island CpG area. Y and R represent T+C and A+G nucleotide, respectively.

1B). The multifocal MSP analysis results are summarized in Table 6. Initially, a methylation density in the different non-tumoral tissues was compared (Fig. 3). The moderate to complete methylation of the *bMLH1* ($p=0.005$) and *Maspin* ($p<0.0001$) CpG islands and the *RABGEF1* non-island CpGs ($p<0.0001$) were significantly higher in the normal lymph nodes than in the gastric mucosa. The low density methylation of the *Maspin* gene at the gastric mucosa of intestinal metaplasia was significantly increased than the gastric mucosa

without intestinal mucosa ($p=0.019$). In contrast, the high density methylation of the *bMLH1* non-island CpGs was significantly increased in the gastric mucosa with intestinal metaplasia as compared with the gastric mucosa without intestinal metaplasia ($p=0.002$). The methylation status of the *CAGE* CpG islands and the *p16* non-island CpGs were similar in the gastric mucosa and lymph nodes.

Table 3. The results of the multifocal microsatellite analysis of gastric carcinomas (n=40)

Case No.	3p	4p	5q	8p	9q	13q	17p	18q	Genotype*	Histological type	Tumor stage
16	■	■	■	■	□	■	■	■	LOH-H	Intestinal type	Stage III
25	■	■	■	□	■	■	■	■	LOH-H	Intestinal type	Stage IV
26	■	■	■	■	■	□	■	■	LOH-H	Intestinal type	Stage III
36	■	□	■	■	■	■	■	■	LOH-H	Mixed type	Stage II
7	□	■	■	■	■	□	■	■	LOH-H	Intestinal type	Stage III
21	■	□	□	■	■	■	■	■	LOH-H	Intestinal type	Stage III
37	■	□	□	■	■	□	■	■	LOH-H	Mixed type	Stage III
38	■	□	■	■	■	■	■	□	LOH-H	Intestinal type	Stage I
3	□	□	■	■	□	□	■	■	LOH-H	Intestinal type	Stage III
29	□	□	□	■	■	■	■	■	LOH-H	Intestinal type	Stage II
24	■	■	■	□	■	■	■	■	LOH-H	Mixed type	Stage IV
48	■	■	□	■	■	□	■	■	LOH-H	Diffuse type	Stage III
50	■	□	■	■	■	■	■	■	LOH-H	Mixed type	Stage IV
41	□	□	■	■	■	■	■	■	LOH-H	Diffuse type	Stage IV
12	□	□	□	■	■	■	■	■	LOH-H	Diffuse type	Stage IV
14	□	□	□	□	■	■	■	■	LOH-H	Diffuse type	Stage III
28	□	□	□	■	□	■	■	■	LOH-H	Intestinal type	Stage II
9	□	□	■	■	□	□	■	□	LOH-L	Mixed type	Stage II
31	■	□	□	□	□	■	■	□	LOH-L	Diffuse type	Stage II
35	□	□	□	■	□	■	■	□	LOH-L	Intestinal type	Stage I
46	□	■	□	□	□	□	■	■	LOH-L	Diffuse type	Stage III
33	□	□	□	□	■	□	■	□	LOH-L	Intestinal type	Stage II
34	□	□	□	□	□	□	■	■	LOH-L	Intestinal type	Stage II
6	□	□	■	□	■	□	■	□	LOH-L	Intestinal type	Stage II
44	□	■	□	□	□	□	■	□	LOH-L	Intestinal type	Stage I
11	■	□	□	■	□	□	□	□	LOH-L	Diffuse type	Stage I
15	□	□	□	□	□	■	■	□	LOH-L	Intestinal type	Stage I
39	□	□	□	□	□	□	□	□	LOH-L	Intestinal type	Stage I
32	■	□	□	□	□	■	□	■	LOH-L	Intestinal type	Stage I
40	□	□	□	■	□	□	■	■	LOH-L	Intestinal type	Stage III
1	□	□	□	■	□	■	□	□	LOH-L	Intestinal type	Stage III
5	■	□	□	□	□	□	□	□	LOH-L	Intestinal type	Stage I
23	□	□	□	□	□	□	□	□	LOH-L	Intestinal type	Stage I
30	□	□	□	□	□	□	■	□	LOH-B	Diffuse type	Stage IV
27	□	□	■	□	□	□	□	□	LOH-B	Diffuse type	Stage III
49	■	□	□	□	□	□	□	□	LOH-B	Diffuse type	Stage II
22	□	□	□	□	□	□	□	□	LOH-B	Mixed type	Stage IV
10	□	□	□	□	□	□	□	□	MSI	Intestinal type	Stage II
2	□	□	□	□	□	□	□	□	MSI	Mixed type	Stage II
43	□	□	□	□	□	□	□	□	MSI	Mixed type	Stage I
(%)	37	24	34	49	47	44	67	53			

*The classification of the microsatellite genotype is detailed in the "Materials and Methods" section. Each rectangle is divided into three parts (□□□) indicating three tumor sites, T1, T2, and T3. ■ constitutional chromosomal loss involving more than one microsatellite marker, □ interstitial chromosomal loss involving one microsatellite marker, ▣ reciprocal loss of upper and lower allele, ▤ positive for microsatellite instability, □ negative for a loss of heterozygosity.

Table 4. Clonality of loss of heterozygosity (LOH) detected by the multifocal analysis on 37 gastric carcinomas

No. of cases	37	Homogeneous LOH (%)	Heterogeneous LOH* (%)	Different losses* (per case)
		24	13	10 (0.77)
Age (yr)				
≤55	10	5 (21)	5 (38)	3 (0.60)
56-65	16	12 (50)	4 (31)	4 (1.00)
>65	11	7 (29)	4 (31)	3 (0.75)
Sex				
Male	24	16 (67)	8 (62)	7 (0.88)
Female	13	8 (33)	5 (38)	3 (0.6)
Tumor size				
≤5 cm	19	10 (42)	9 (69)	7 (0.78)
>5 cm	18	14 (58)	4 (31)	3 (0.75)
Histological type				
Intestinal	21	16 (66)	5 (39)	3 (0.60)
Diffuse	10	4 (17)	6 (46)	5 (0.83)
Mixed	6	4 (17)	2 (15)	2 (1.00)
Tumor stage				
Early stage	18	14 (58)	4 (31)	1 (0.25)
Advanced stage	19	10 (42)	9 (69)	9 (1.00)
Chromosomal loss				
Baseline level	4	2 (8)	2 (15)	1 (0.50)
Low level	16	12 (50)	4 (31)	2 (0.50)
High level	17	10 (42)	7 (54)	7 (1.00)

*The reciprocal loss of the upper and lower opposite alleles on the same chromosomes was not counted as a different chromosomal loss.

Comparison of methylation density between the paired normal and tumor tissues

When comparing the methylation status of the nontumoral gastric mucosa and their corresponding heterogeneous tumor sites (Fig. 3), the zero to two methylation of the CpG islands of the *Maspin* ($p=0.031$) and *CAGE* ($p=0.005$) genes as well as the non-island CpGs of the *MAGE-A2* ($p<0.0001$) and *RABGEF1* ($p=0.004$) genes was significantly higher in the tumor tissues. The tumor tissues demonstrated significant increases in the methylation density at the *bMLH1* ($p=0.020$), *p16* ($p=0.005$), and *RASSF1A* ($p=0.015$) CpG islands that were completely unmethylated in the normal tissues. The CpG islands of the *RABGEF1*, *p15* and *E-cadherin* genes suffered few methylation differences in tumor tissues.

The methylation status of the tumor tissues was analyzed separately according to the four microsatellite genotypes, LOH-H, LOH-L, LOH-B, and MSI (Fig. 3). The methylation density at the CpG islands of the *Maspin* ($p=0.007$) and *CAGE* ($p=0.010$) genes in addition to all of the non-island CpGs upstream of the *p16* ($p=0.013$), *bMLH1* ($p=0.003$), *MAGE-A2* ($p<0.0001$) and *RABGEF1* ($p<0.0001$) genes were significantly decreased in the LOH-H tumor sites. The LOH-L tumor sites showed significant increased methylation in the CpG islands of the *bMLH1* ($p=0.012$), *RASSF1A* ($p=0.037$), *p16* ($p=0.049$) and *Cyclin D2* ($p=0.034$) genes, and

Table 5. Clinicopathological characteristics of microsatellite genotypes in gastric carcinomas

Microsatellite genotype*	33	LOH-H	LOH-L	p value†	LOH-B	MSI
No. of patients		17	16		4	3
Age (yr)				0.507		
Mean ± SD	60.1 ± 10.8	61.4 ± 10.1	58.5 ± 11.6		53.3 ± 7.4	69.0 ± 13.5
Tumor size, cm				0.409		
Mean ± SD	5.3 ± 2.7	5.7 ± 2.5	4.9 ± 2.8		4.92 ± 2.6	8.5 ± 4.4
Sex				0.451		
Male	22	12	10		2	1
Female	11	5	6		2	2
Location				0.249		
Cardia	2	0	2		0	0
Body	7	3	4		4	0
Antrum	24	14	10		0	3
Lauren classification				0.310		
Intestinal	21	9	12		0	1
Diffuse	7	4	3		3	0
Mixed	5	4	1		1	2
Differentiation				0.084		
Well	4	0	4		0	0
Moderate	18	11	7		0	1
Poor	11	6	5		4	2
Growth pattern				0.282		
Infiltrative	22	13	9		1	1
Expanding	0	0	0		0	1
Mixed	13	4	7		3	1
Venous invasion				0.227		
Yes	3	3	0		2	0
No	30	14	16		2	3
Lymphatic invasion				0.005		
Yes	19	14	5		4	2
No	14	3	11		0	1
Tumor stage				0.002		
Early stage	17	4	13		1	3
Advanced stage	16	13	3		3	0

*The classification of microsatellite genotypes is detailed in the "Materials and Methods" section. † p -values were calculated between the LOH-L and LOH-H cases by an independent t-test for the age and tumor size variables and by a Fisher's exact test or a χ^2 -test for the other variables.

in the non-island CpGs of the *p16* ($p=0.038$) and *bMLH1* ($p=0.005$) genes. The increased methylation density of the six CpG regions in the LOH-L cases was significantly different from the unchanged (CpG islands) or decreased (non-island CpGs) methylation density in the LOH-H cases. All the p -values are listed in the Table 7.

In both the LOH-B and MSI cases, the methylation density tended to be higher in the CpG islands of the *RASSF1A*, *p16*, and *Cyclin D2* genes as well as in the non-island CpGs of the *p16* and *bMLH1* genes. The CpG islands of the *bMLH1* gene were mainly hypermethylated in the nine tumor sites from the three MSI-positive cases (complete methylation in 8 tumor sites and incomplete methylation in 1 tumor sites). Unmethylated *E-cadherin* CpG islands were detected in the

Table 6. Summary of the multifocal methylation analysis on gastric carcinomas

Case No.	CpG island									Non-island CpG			
	RABGEF1	hMLH1	RASSF1A	Maspin	p16	Cyclin D2	CAGE	p15	E-cadherin	p16	hMLH1	RABGEF1	MAGE-A2
16													
25													
26													
36													
7													
21													
37													
38													
3													
29													
24													
48													
50													
41													
12													
14													
28													
9													
31													
35													
46													
33													
34													
6													
44													
11													
15													
39													
32													
40													
1													
5													
23													
30													
27													
49													
22													
10													
2													
43													

The methylation status of each case is indicated by five parts in the order of the lymph node, normal mucosa, and the three tumor sites. □ 0-20% methylation, ▤ 21-40% methylation, ▥ 41-60% methylation, ▧ 61-80% methylation, ▩ 81-100% methylation.

LOH-B and MSI cases. The statistical analysis results are not shown for the small number of LOH-B and MSI cases.

Relationships between the methylation differences and the clinicopathological features

A difference in the methylation density between the paired nontumoral gastric mucosa and each tumor site was graded U1 through to U4 according to the decreased methylation

degree and M1 through to M4 according to the increased methylation degree. The mean value of the methylation differences in the three tumor sites was correlated with the clinicopathological features in a subset of gastric carcinomas with low- and high-level chromosomal losses (Table 8). The *hMLH1* ($p=0.034$), *RASSF1A* ($p=0.031$), and *p16* ($p=0.031$) CpG islands and the four non-island CpGs (*p16*, $p=0.002$; *hMLH1*, $p<0.0001$; *RABGEF1*, $p=0.015$; *MAGE-A2*, $p<0.0001$) showed statistical significances in the pattern of methylation

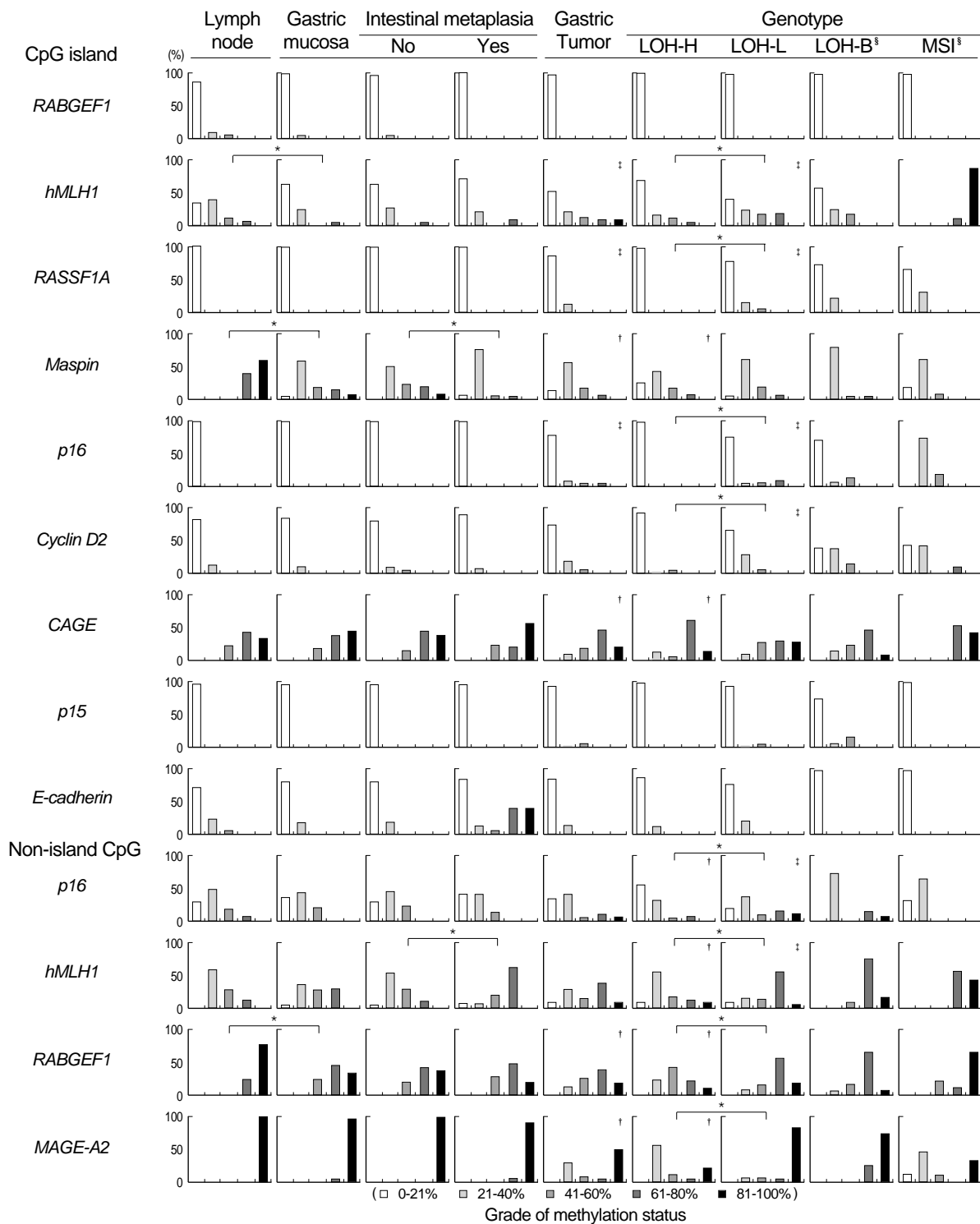


Fig. 3. Methylation profiles of the CpG islands and non-island CpGs in the nontumoral and tumoral tissues. The nontumoral gastric mucosa is grouped according to the presence and absence of the intestinal metaplasia. The tumor tissues are grouped into four microsatellite genotypes. The classification of the microsatellite genotypes is detailed in the “Materials and Methods” section. The CpG methylation status in each tissue group is given as a percentage of five grades. The *p*-value was calculated using the Mann-Whitney *U* test. There were *significant differences in methylation density between the lymph node and gastric mucosa, between the presence and absence of intestinal metaplasia, and between the LOH-H and LOH-L groups. The heterogeneous tumor sites showed significant †decreased methylation and ‡increased methylation density compared with the gastric mucosa. §Statistical comparison was not shown due to the small number of LOH-B and MSI cases. All *p*-values are listed in the Table 7.

Table 7. P values of the statistical analysis presented in Figure 3

	Lymph node vs. gastric mucosa	Intestinal metaplasia No vs. yes	Gastric mucosa vs. Tumor	Gastric mucosa vs. LOH-H genotype tumor	Gastric mucosa vs. LOH-L genotype tumor	LOH-H vs. LOH-L genotype tumor
CpG island						
<i>RABGEF1</i>	0.088	0.463	0.380	0.360	1.000	0.359
<i>hMLH1</i>	0.005*	0.769	0.020*	0.639	0.012*	0.001*
<i>RASSF1A</i>	1.000	1.000	0.015*	1.000	0.037*	<0.0001*
<i>Maspin</i>	<0.0001*	0.019*	0.031*	0.007*	0.567	0.197
<i>p16</i>	1.000	1.000	0.005*	1.000	0.049*	<0.0001*
<i>Cyclin D2</i>	0.784	0.444	0.114	0.096	0.034*	<0.0001*
<i>CAGE</i>	0.362	0.499	0.005*	0.010*	0.263	0.867
<i>p15</i>	1.000	1.000	0.132	0.582	0.310	0.233
<i>E-cadherin</i>	0.151	0.698	0.562	0.713	0.463	0.080
Non-island CpG						
<i>p16</i>	0.707	0.392	0.695	0.013*	0.038*	<0.0001*
<i>hMLH1</i>	0.142	0.002*	0.211	0.003*	0.005*	<0.0001*
<i>RABGEF1</i>	<0.0001*	0.279	0.004*	<0.0001*	0.455	<0.0001*
<i>MAGE-A2</i>	0.317	0.173	<0.0001*	<0.0001*	0.084	<0.0001*

*p values <0.05.

differences between the LOH-H and LOH-L cases.

In a subset of gastric carcinomas with low-level or high-level chromosomal losses, the decreased methylation differences in the non-island CpGs of *p16*, *hMLH1*, and *MAGE-A2* genes correlated with the mixed histological type, a lymphatic invasion, and an advanced tumor stage ($p < 0.05$) (Table 8). The decreased methylation differences in the CpG islands of the *Maspin* genes were associated with the large-sized tumors ($p = 0.012$). In contrast, the increased methylation differences in the *p16* CpG islands correlated with well differentiation ($p = 0.039$), a small size ($p = 0.042$), a non-lymphatic invasion ($p = 0.031$) and an early tumor stage ($p = 0.042$). The relationships between the increased methylation differences in the CpG islands other than *p16* and either a non-lymphatic invasion (*hMLH1*, $p = 0.035$; *RASSF1A*, $p = 0.031$) or an early tumor stage (*RASSF1A*, $p = 0.042$) also reached borderline-level statistical significance.

Methylation heterogeneity

A total of 1,560 pairs of methylation and unmethylation bands were obtained from the 120 heterogeneous tumor sites using MSP analysis on the 13 CpG regions, of which 305 (19%), 267 (17%), and 991 (64%) demonstrated decreased methylation, increased methylation, and no methylation changes, respectively. When analyzing the pattern and grade of methylation differences in three heterogeneous sites of each case (Fig. 4A), the grade of increased and decreased methylation differences were similar (8% and 11%) or dissimilar (12% and 11%). However, no gastric carcinomas showed both the increased and decreased methylation in heterogeneous tumor sites simultaneously.

A large fraction (59%) of methylation differences tended to cluster in a range of U1 and M1 low-grade differences,

whereas a complete difference (M4 and U4) of the methylation status was detected in only five normal mucosa-tumor pairs (0.9%) (Fig. 4B). The three tumor-cell-content groups, 70-79% (221 tumor sites), 80-89% (962 tumor sites), and $\geq 90\%$ (377 tumor sites), demonstrated varying grades of methylation differences (Fig. 4C). The U1 and M1 low-grade differences and the U3 and M3 high-grade differences were similarly increased in the high tumor-cell-content group (63% and 12%) when compared with the low tumor-cell-content group (57% and 8%).

The CpG islands and non-island CpGs of the *p16*, *hMLH1*, and *MAGE-A2* genes were amplified and cloned using the methylation-unmethylation common primers encompassing the MSP primer sequences (Fig. 5). The methylation densities of the individual PCR clones examined using the MSP primer sets were different (Fig. 5A), and the number and position of the methylated CpGs identified by bisulfite sequencing were heterogeneous (Fig. 5B). The pooled PCR clones showed a similar proportion of methylated and unmethylated amplifications to the corresponding genomic DNA (Fig. 5A).

DISCUSSION

The aforementioned studies have reported frequent gene-specific hypermethylation in the intestinal metaplasia and adenoma (15), whereas chromosomal losses were rare in the intestinal metaplasia and low-grade dysplasia (25). Given the multistep carcinogenesis, the tumor progenitor cells acquiring the hypermethylation in the initial step appear to subclonally expand via further hypermethylation or chromosomal losses (genome dosage reduction) providing a selective growth advantage. The previous results that <10% of colorectal carcinomas show frequent methylation of the CpG

Table 8. Relationships between the methylation differences and either the genotype or the clinocopathological features in a subset of gastric carcinomas with low-level (16 cases) and high-level (17 cases) chromosomal losses

	CpG island									Non-island CpG			
	<i>RABGEF1</i>	<i>hMLH1</i>	<i>RASSF1A</i>	<i>Maspin</i>	<i>p16</i>	<i>Cyclin D2</i>	<i>CAGE</i>	<i>p15</i>	<i>E-cadherin</i>	<i>p16</i>	<i>hMLH1</i>	<i>RABGEF1</i>	<i>MAGE-A2</i>
Genotype													
High-level	U0.06	U0.06	0	U0.82	0	U0.12	U0.71	0	U0.00	U0.71	U0.71	U1.00	U2.12
Low-level	0	M0.75	M0.31	U0.13	M0.56	M0.25	U0.25	M0.13	M0.06	M0.88	M0.88	U0.13	U0.38
<i>p</i> value	0.332	0.034*	0.031*	0.077	0.031*	0.120	0.199	0.303	0.665	0.002*	< 0.0001*	0.015*	< 0.0001*
Age													
≤55	U0.13	M0.25	0	U0.37	0	U0.13	U0.25	0	M0.13	U0.13	M0.13	U0.63	U1.38
56-65	0	M0.36	M0.07	U0.64	M0.57	M0.07	U0.71	M0.14	0	M0.21	M0.14	U0.36	U1.21
> 65	0	M0.36	M0.36	U0.36	M0.09	M0.18	U0.36	0	0	M0.36	U0.09	U0.82	U1.27
<i>p</i> value	0.210	0.984	0.151	0.919	0.291	0.780	0.545	0.507	0.721	0.710	0.974	0.651	0.883
Sex													
Male	0	M0.09	M0.09	U0.36	M0.36	M0.18	U0.50	M0.09	M0.09	M0.05	U0.09	U0.64	U1.36
Female	U0.09	M0.82	M0.27	U0.72	M0.09	U0.18	U0.45	0	U0.09	M0.45	M0.36	U0.45	U1.09
<i>p</i> value	0.157	0.121	0.418	0.237	0.637	0.184	0.858	0.480	0.220	0.439	0.467	0.492	0.627
Lauren classification													
Intestinal	0	M0.52	M0.24	U0.33	M0.43	M0.19	U0.67	M0.09	M0.10	M0.57	M0.38	U0.48	U1.10
Diffuse	U0.14	M0.29	0	U0.42	0	U0.29	M0.43	0	U0.29	U0.43	M0.28	U0.57	U0.57
Mixed	0	U0.40	0	U1.20	0	0	U0.20	0	M0.20	U0.60	U1.60	U1.00	U3.00
<i>p</i> value	0.156	0.192	0.284	0.498	0.285	0.172	0.388	0.751	0.052	0.043*	0.020*	0.560	0.011*
Differentiation													
Well	0	M0.25	M0.25	M0.25	M1.00	M0.50	0	0	M0.25	M1.25	M1.00	0	0
Moderate	0	M0.33	M0.17	U0.50	M0.28	M0.17	U0.78	M0.11	M0.06	M0.16	U0.33	U0.61	U1.78
Poor	U0.09	M0.36	M0.09	U0.64	0	U0.27	U0.18	0	U0.09	U0.18	M0.36	U0.73	U0.91
<i>p</i> value	0.368	1.000	0.723	0.348	0.039*	0.093	0.200	0.659	0.314	0.123	0.148	0.352	0.045*
Tumor size													
≤5 cm	0	M0.53	M0.12	0	M0.53	M0.24	U0.71	M0.12	M0.06	M0.35	M0.29	U0.59	U1.12
> 5 cm	U0.06	M0.13	M0.19	U1.00	0	U0.13	U0.25	0	M0.01	U0.01	U0.19	U0.56	U1.44
<i>p</i> value	0.303	0.183	0.899	0.012*	0.042*	0.136	0.288	0.332	0.665	0.389	0.221	0.819	0.536
Lymphatic invasion													
Yes	U0.05	U0.05	0	U0.68	0	U0.11	U0.47	0	U0.05	U0.37	U0.42	U0.84	U1.95
No	0	M0.77	M0.31	U0.31	M0.54	M0.23	U0.46	0	M0.15	M0.92	M0.62	U0.15	U0.38
<i>p</i> value	0.408	0.035*	0.031*	0.669	0.031*	0.152	0.936	1.000	0.153	0.006*	0.017*	0.078	0.002*
Stage													
Early	0	M0.65	M0.29	U0.47	M0.53	M0.12	U0.35	M0.12	M0.18	M0.82	M0.53	U0.24	U0.65
Advanced	U0.06	M0.00	0	U0.50	0	U0.00	U0.63	0	U0.13	U0.50	U0.44	U0.94	U1.94
<i>p</i> value	0.303	0.099	0.042*	0.758	0.042*	0.387	0.442	0.332	0.179	0.002*	0.023*	0.070	0.006*

A mean value of the increased methylation (M1-4) or decreased methylation (U1-4) differences in each genotype or phenotype group was calculated based on methylation differences between one normal site and three tumor sites in each case. **p* values <0.05.

islands at the methylated-in-tumor (MINT) loci, but no MSI, which is associated with a poor prognosis (16). In this study, the four LOH-B cases detected in 10% of gastric carcinomas examined, which have been reported to be associated with poor prognosis (7, 8), shows a tendency toward an increase in methylation density. These findings on colon and gastric carcinomas similarly suggest that a subset of high-risk gastric carcinomas develop largely depending on methylator phenotype.

The methylation density at the CpG islands of the *Maspin* and *CAGE* genes as well as the non-island CpGs of the *MAGE-A2* and *RABGEF1* genes were decreased in the tumor tissues, which were significantly different from the normal tissues (Fig. 3) in similarity with previous studies (24, 26, 27). A

tendency toward decreased methylation differences in these CpG islands and non-island CpGs was found to be significantly associated with the LOH-H cases but not with the LOH-L cases (Table 8). Interestingly, the methylation differences at the non-island CpGs of the *p16* and *hMLH1* genes that were incompletely methylated in the normal tissues tended to be decreased in the LOH-H cases, and they were further increased in LOH-B, LOH-L, and MSI cases (Fig. 6). The extragenic regions upstream of a gene appear to formulate a distance-dependent methylation gradient, which is easily dislodged for hypomethylation as well as hypermethylation. The hypomethylation compensating for the chromosomal losses can explain why the MSI inversely correlates with the chromosomal losses (7, 28). This inverse relationship might

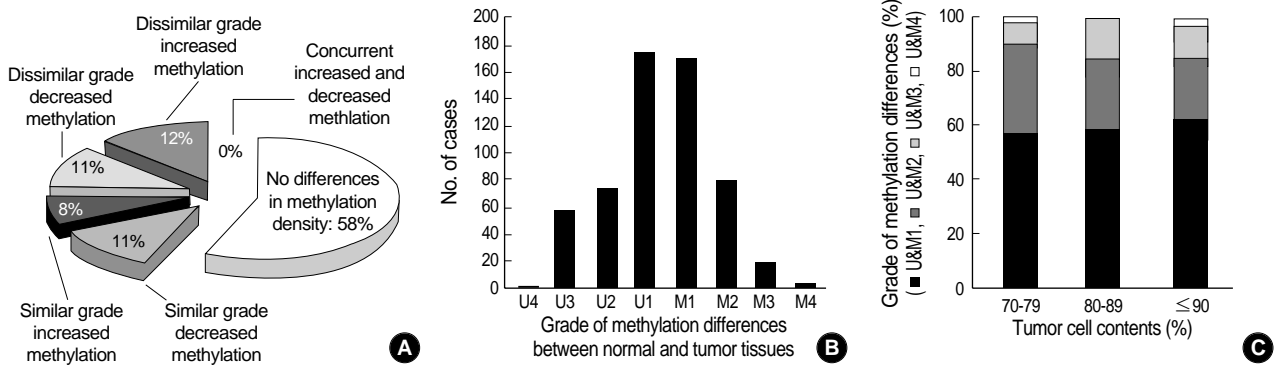


Fig. 4. Methylation heterogeneity on gastric carcinomas detected by multifocal analysis. The methylation status of the 13 CpG regions is detailed in Table 6. (A) The grade and pattern of the methylation differences in a given CpG region in different tumor sites from a given gastric carcinoma were compared. (B) The methylation differences detected in individual tumor sites are shown separately according to the grade of the methylation differences. (C) The grades of the methylation differences given as percentage were compared between different tumor-cell-content groups. The differences in the methylated-unmethylated proportion between the paired normal and heterogeneous tumor sites were graded U1-U4 decreased methylation differences and M1-M4 increased methylation differences.

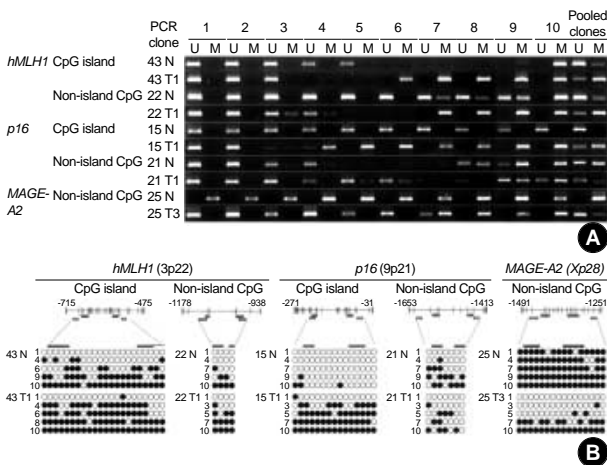


Fig. 5. Heterogeneous methylation profiles of the *p16*, *hMLH1*, and *MAGE-A2* CpG regions. PCR products common for methylated and unmethylated CpGs were cloned and ten clones were randomly selected. The individual and pooled clones were amplified by the MSP primer sets (A). The individual PCR clones generated heterogeneous methylation densities in the MSP analysis. The pooled PCR clones showed similar MSP patterns with those of the corresponding genomic DNAs listed in Table 6. Five PCR clones from each genomic DNA generating different or no MSP band intensities were sequenced (B). PCR primers specific for the unmethylation (≡) and methylation (■), and common (≡) for the methylation and unmethylation are indicated by the horizontal bars below the vertical lines marking the individual CpG sites. Individual CpG sites of each PCR clone are indicated as circles in a clone-numbered row. A closed circle marks a methylated CpG and an open circle marks an unmethylated CpG. The methylation composition of the PCR clones was heterogeneous in similarity with a broad range of methylated and unmethylated band intensities. One or two primer-template sequence mismatches produced weak band intensities. Multiple sequence mismatches in the primer regions of the *hMLH1* CpG islands (normal clone 6 and tumor clone 4 in case 43) produced none of the methylation and unmethylation bands.

result from the hypomethylation effect of chromosomal loss on the *bMLH1* promoter region in which hypermethylation silence the mismatch repair gene and induce the MSI.

The methylation density at the non-island CpGs of the *RABGEF1* gene arbitrarily selected in this study was significantly decreased in the LOH-H cases but there was no significant relationship with the clinicopathological features. Given the genome-wide influence of a dosage compensation mechanism that maintains the X-to-autosomal chromosome ratio (10, 11), the hypomethylation can occur in the cancer-related as well as cancer-unrelated genes in association with high-level chromosomal losses. Therefore, the high-grade hypomethylation compensating for the high-level dosage reduction are likely to surpass the initial hypermethylation and to drive the progression of high-risk gastric carcinomas independent of the hypermethylation status (Fig. 7). This supports the previous study of colorectal cancer that hypermethylation and hypomethylation separately contribute to the process of carcinogenesis (29).

The increased methylation differences in the *p16*, *bMLH1*, and *RASSF1A* CpG islands were statistically significant at well differentiation, no lymphatic invasion, and the early tumor stage (Table 8). The same increased methylation differences observed frequently in both the LOH-B and LOH-L cases were paradoxical, because the two genotypes represent high-risk and low-risk gastric carcinomas, respectively (Fig. 3). Moreover, the decreased methylation differences in the non-island CpGs adjacent to the *p16* and *bMLH1* genes were associated with the advanced tumor stage and a lymphatic invasion (Table 8). These paradoxical relationships between epigenetic alterations and malignant phenotypes can be explained by the dynamic pathways composed of preceding hypermethylation, irreversible chromosomal loss, and compensative hypomethylation. The gene-specific hypermethylation changes may initiate the tumor formation in a precancerous lesion

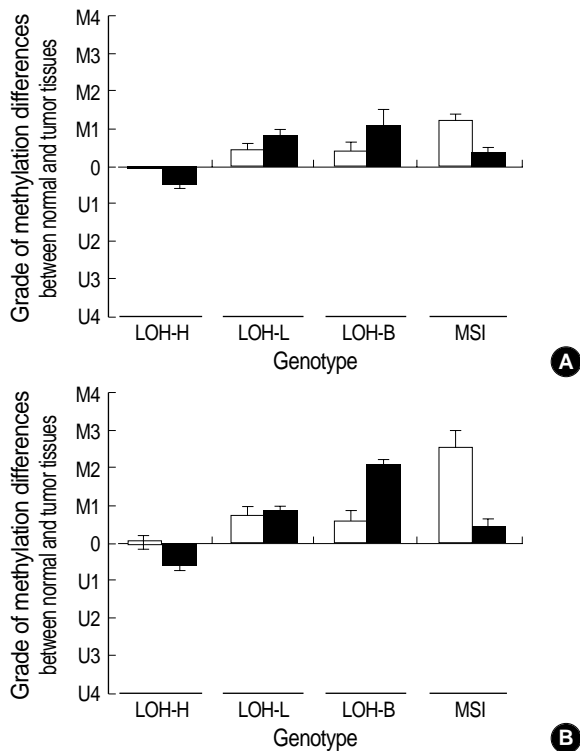


Fig. 6. Pattern of methylation differences in the CpG island (□) and non-island CpG (■) area of the *p16* (A) and *hMLH1* (B) genes. The gastric carcinoma was classified as four microsatellite genotypes. The classification of the microsatellite genotypes is detailed in the “Materials and Methods” section. The decreased methylation differences in the LOH-L cases and the increased methylation differences in the LOH-H, LOH-B, and MSI cases were observed in the methylation gradient region between the CpG islands and non-island CpG area of the same gene. The increased methylation (M1-4) and decreased methylation (U1-4) differences are indicated by a difference in methylation grade between the gastric mucosa and the gastric carcinoma. The bar and error bar represents the mean and SEM of the methylation grade difference.

and/or be potentially associated with the hypermethylation-dependent LOH-B cases (15, 16). The high-level chromosomal losses stimulate the hypomethylation-dependent pathway requiring no hypermethylation. The low-grade hypomethylation compensating for the LOH-L cases is thought to attenuate the extent of hypermethylation at high risk (Fig. 7). Alternatively, the low-level chromosomal losses are likely to cooperate with the hypermethylation for the development and progression of a low-risk gastric carcinoma.

It should be noted that multidirectionally differentiated mixed cancers such as a sarcomatoid carcinoma (30) and a glandular-neuroendocrine carcinoma (31) as well as heterogeneous tumor sites of a gastric carcinoma commonly have divergent losses involving different alleles on the same chromosome. Considering that epigenetic changes occur only in dividing cells (32), the divergent losses bifurcated in mixed tumors suggest that a genome dosage reduction results in the gradual and heterogeneous hypomethylation during car-

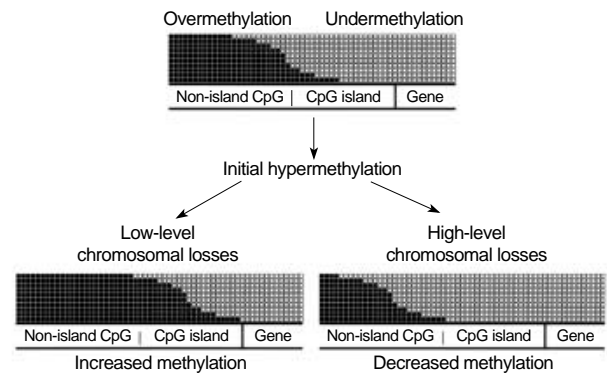


Fig. 7. Schematic illustration of the CpG methylation status dislodged dependent on the extent of chromosomal losses. A methylation gradient between the undermethylated CpG-rich promoter region (CpG island) and the overmethylated CpG-poor region (non-island CpG) is prone to both hypo- and hypermethylation. The high-level (LOH-H) and low-level (LOH-L) chromosomal losses stimulate the variable hypomethylation in the methylation-gradient regions via dosage-compensation mechanism. Significant hypomethylation in the LOH-H cases demethylate the initial hypermethylation, leading to few hypermethylation. Meanwhile, the LOH-L cases are under the influence of low-grade hypomethylation and retain the initial methylation changes.

cinogenesis, which give rise to the expansion of dissimilar subclones driven by the same chromosomal loss.

Assuming the compensative interactions between the chromosomal losses and the methylation changes maintain a genomic dosage, the extent of irreversible chromosomal losses and the pattern of reversible methylation are likely to be stable and are unlikely to progress from the LOH-L cases to the LOH-H or LOH-B cases. In a previous LOH study using the same microsatellite markers (8), a lymph node metastasis and extraserosal invasion were frequent irrespective of the tumor size in the LOH-H and LOH-B cases. In contrast, in the LOH-L cases, the rate of a lymph node metastasis and extraserosal invasion increased linearly with the increased tumor size. The age of onset and the tumor size in the LOH-L and LOH-H cases, which were significantly associated with the early and advanced tumor stage, respectively, were similar (Table 8). It is likely that the clinical course of a gastric carcinoma is determined at the early stage and is dependent on the stem-line extent of chromosomal losses before tumor cells appear as a visible mass.

The MSI cases demonstrated frequent hypermethylation and infrequent hypomethylation (Fig. 3), which is in agreement with a subset of gastric carcinomas positive for MSI and MINT (15, 33). The MSI cases associated with a good prognosis contain many cancer-related mutations caused by hypermethylation silencing the mismatch repair gene. The accumulation of irreversible gene mutation might be disadvantageous over the viable tumor cells due to the lack of a physiological gene function. Unlike the reversible methylator phenotype, the irreversible mutator phenotype appears to lead to a favorable clinical course.

The present methylation analysis of the paired normal and tumor tissues identified an epigenetic heterogeneity in the CpG islands as well as in the non-island CpGs adjacent to the cancer-related and -unrelated genes. A complete conversion of the methylation status in the tumor tissues was quite rare in the CpG sites examined (Fig. 4B). A high tumor cell contents $\geq 90\%$ tended to increase both the low- and high-grade methylation differences (Fig. 4C). The amplification intensity of the MSP analysis along with the methylated CpG composition identified by bisulfite sequencing also showed a wide range of methylation densities in the CpG islands and non-island CpGs (Fig. 5). Previous bisulfite sequencing analyses on tumor cell lines and pure primary tissues have also reported a wide range of methylation densities in the CpG island regions of the *Maspin*, *CAGE*, *E-cadherin*, *p16*, and *bMLH1* genes (26, 27, 34-36). This indicates that the heterogeneous methylation changes in the 5'-flanking regions were generalized over the tumor tissues.

The hypermethylation status in the CpG islands examined in this study were extensively examined in previous studies on gastric carcinomas, and the rates reported in the literature varied from 10% to as high as 67% for the *p16* CpG island (37, 38) and from 18% to 33% for the *bMLH1* CpG island (33, 39). Moreover, the CpG island hypermethylation was also observed in 0-67% of the normal gastric mucosa (15, 39). In this study, the incompletely unmethylated CpG island of the *bMLH1* gene (33%) was frequently methylated (48%) and completely unmethylated CpG islands of the *p16* and *RASSF1A* genes were slightly methylated (18% and 14%). The methylation differences between gastric mucosa and tumor were more prominent in variably methylated non-island CpGs than relatively unmethylated CpG islands of the *bMLH1* and *p16* genes (Fig. 6). The normal lymph nodes contained an increased methylated density in the CpG islands of the *bMLH1* and *Maspin* genes and the non-island CpGs of the *RABGEF1* gene compared with the normal gastric mucosa (Fig. 3). The wide hypermethylation rates might be caused by the genomic position of the CpG sites examined and the cell content of the normal and tumor tissues.

The number of PCR cycles is important for an unbiased amplification of the bisulfite-modified heterogeneous sequences. This study performed a minimum number of 32 PCR cycles using a radioisotope for the slightly erroneous PCR products. The heterogeneous tumor tissues in each case tended to have a pattern of increased or decreased methylation differences, but not both differences, in a CpG region that was dependent on the stem-line extent of chromosomal losses (Fig. 4A). Only one case (case 28) contained low-level (two) and high-level (four) chromosomal losses as well as a similar methylation pattern in the heterogeneous sites. These findings support a close relationship between the chromosomal loss and the heterogeneous methylation differences. The biased MSP condition is unlikely given to the pattern of methylation differences measured in the paired normal and tumor tissues.

This multifocal genetic and epigenetic study on gastric carcinomas can explain the tumor progression process based on the stem-line chromosomal losses and the compensative or cooperative reversible epigenetic changes. The extent of the chromosomal losses is believed to drive the diverse progression of a gastric carcinoma via a dosage compensative mechanism that influences the methylation status of the tumor cells.

REFERENCES

- Balmain A, Gray J, Ponder B. *The genetics and genomics of cancer. Nat Genet* 2003; 33: 238-44.
- Lasko D, Cavenee W, Nordenskjold M. *Loss of constitutional heterozygosity in human cancer. Annu Rev Genet* 1991; 25: 281-314.
- Vogelstein B, Fearon ER, Kern SE, Hamilton SR, Preisinger AC, Nakamura Y, White R. *Allelotype of colorectal carcinomas. Science* 1989; 244: 207-11.
- Choi SW, Lee KJ, Bae YA, Min KO, Kwon MS, Kim KM, Rhyu MG. *Genetic classification of colorectal cancer based on chromosomal loss and microsatellite instability predicts survival. Clin Cancer Res* 2002; 8: 2311-22.
- Nagel S, Borisch B, Thein SL, Oestreicher M, Nothiger F, Birrer S, Tobler A, Fey MF. *Somatic mutations detected by mini- and microsatellite DNA markers reveal clonal intratumor heterogeneity in gastrointestinal cancers. Cancer Res* 1995; 55: 2866-70.
- Chung YJ, Choi JR, Park SW, Kim KM, Rhyu MG. *Evidence for two modes of allelic loss: multifocal analysis on both early and advanced gastric carcinomas. Virchows Arch* 2001; 438: 31-8.
- Kim KM, Kwon MS, Hong SJ, Min KO, Seo EJ, Lee KY, Choi SW, Rhyu MG. *Genetic classification of intestinal-type and diffuse-type gastric cancers based on chromosomal loss and microsatellite instability. Virchows Arch* 2003; 443: 491-500.
- Hong SJ, Choi SW, Lee KH, Lee S, Min KO, Rhyu MG. *Preoperative genetic diagnosis of gastric carcinoma based on chromosomal loss and microsatellite instability. Int J Cancer* 2005; 113: 249-58.
- Meller VH. *Dosage compensation: making 1X equal 2X. Trends Cell Biol* 2000; 10: 54-9.
- Muller H. *Why polyploid is rarer in animals than in plants. American Nature* 1925; 59: 346-53.
- Gallardo MH, Bickham JW, Honeycutt RL, Ojeda RA, Kohler N. *Discovery of tetraploidy in a mammal. Nature* 1999; 401: 341.
- Ehrlich M. *DNA methylation in cancer: too much, but also too little. Oncogene* 2002; 21: 5400-13.
- Lin CH, Hsieh SY, Sheen IS, Lee WC, Chen TC, Shyu WC, Liaw YF. *Genome-wide hypomethylation in hepatocellular carcinogenesis. Cancer Res* 2001; 61: 4238-43.
- Henikoff S. *Heterochromatin function in complex genomes. Biochim Biophys Acta* 2000; 1470: 1-8.
- Lee JH, Park SJ, Abraham SC, Seo JS, Nam JH, Choi C, Juhng SW, Rashid A, Hamilton SR, Wu TT. *Frequent CpG island methylation in precursor lesions and early gastric adenocarcinomas. Oncogene* 2004; 23: 4646-54.

16. Ward RL, Cheong K, Ku SL, Meagher A, O'Connor T, Hawkins NJ. Adverse prognostic effect of methylation in colorectal cancer is reversed by microsatellite instability. *J Clin Oncol* 2003; 21: 3729-36.
17. Yang AS, Estecio MR, Garcia-Manero G, Kantarjian HM, Issa JP. Comment on "Chromosomal instability and tumors promoted by DNA hypomethylation" and "Induction of tumors in mice by genomic hypomethylation". *Science* 2003; 302: 1153.
18. Lauren P. The two histological main types of gastric carcinoma: diffuse and so-called intestinal-type carcinoma. *Acta Pathol Microbiol Scand* 1965; 64: 31-49.
19. Greene FL, Page DL, Fleming ID, Fritz A, Balch CM, Haller DG, Morrow M. *AJCC cancer staging manual*. Berlin Heidelberg New York: Springer Verlag, 2002.
20. Clark SJ, Harrison J, Paul CL, Frommer M. High sensitivity mapping of methylated cytosines. *Nucleic Acids Res* 1994; 22: 2990-7.
21. Herman JG, Umar A, Polyak K, Graff JR, Ahuja N, Issa JP, Markowitz S, Willson JK, Hamilton SR, Kinzler KW, Kane MF, Kolodner RD, Vogelstein B, Kunkel TA, Baylin SB. Incidence and functional consequences of hMLH1 promoter hypermethylation in colorectal carcinoma. *Proc Natl Acad Sci USA* 1998; 95: 6870-5.
22. Lo KW, Kwong J, Hui AB, Chan SY, To KF, Chan AS, Chow LS, Teo PM, Johnson PJ, Huang DP. High frequency of promoter hypermethylation of RASSF1A in nasopharyngeal carcinoma. *Cancer Res* 2001; 61: 3877-81.
23. Herman JG, Graff JR, Myohanen S, Nelkin BD, Baylin SB. Methylation-specific PCR: a novel PCR assay for methylation status of CpG islands. *Proc Natl Acad Sci USA* 1996; 93: 9821-6.
24. Kaneda A, Tsukamoto T, Takamura-Enya T, Watanabe N, Kaminishi M, Sugimura T, Tatematsu M, Ushijima T. Frequent hypomethylation in multiple promoter CpG islands is associated with global hypomethylation, but not with frequent promoter hypermethylation. *Cancer Sci* 2004; 95: 58-64.
25. Kokkola A, Monni O, Puolakkainen P, Nordling S, Haapiainen R, Kivilaakso E, Knuutila S. Presence of high-level DNA copy number gains in gastric carcinoma and severely dysplastic adenomas but not in moderately dysplastic adenomas. *Cancer Genet Cytogenet* 1998; 107: 32-6.
26. Akiyama Y, Maesawa C, Ogasawara S, Terashima M, Masuda T. Cell-type-specific repression of the maspin gene is disrupted frequently by demethylation at the promoter region in gastric intestinal metaplasia and cancer cells. *Am J Pathol* 2003; 163: 1911-9.
27. Cho B, Lee H, Jeong S, Bang YJ, Lee HJ, Hwang KS, Kim HY, Lee YS, Kang GH, Jeoung DI. Promoter hypomethylation of a novel cancer/testis antigen gene CAGE is correlated with its aberrant expression and is seen in premalignant stage of gastric carcinoma. *Biochem Biophys Res Commun* 2003; 307: 52-63.
28. Martin L, Assem M, Piard F. Are there several types of colorectal carcinomas? Correlations with genetic data. *Eur J Cancer Prev* 1999; 8 (Suppl 1): 13-20.
29. Bariol C, Suter C, Cheong K, Ku SL, Meagher A, Hawkins N, Ward R. The relationship between hypomethylation and CpG island methylation in colorectal neoplasia. *Am J Pathol* 2003; 162: 1361-71.
30. Kwon MS, Hong SJ, Cho HA, Ahn GH, Lee SS, Lee KY, Rhyu MG. Extensive and divergent chromosomal losses in squamous and spindle-cell components of esophageal sarcomatoid carcinoma. *Virchows Arch* 2003; 443: 635-42.
31. Kim KM, Kim MJ, Cho BK, Choi SW, Rhyu MG. Genetic evidence for the multi-step progression of mixed glandular-neuroendocrine gastric carcinomas. *Virchows Arch* 2002; 440: 85-93.
32. Velicescu M, Weisenberger DJ, Gonzales FA, Tsai YC, Nguyen CT, Jones PA. Cell division is required for de novo methylation of CpG islands in bladder cancer cells. *Cancer Res* 2002; 62: 2378-84.
33. Oue N, Oshimo Y, Nakayama H, Ito R, Yoshida K, Matsusaki K, Yasui W. DNA methylation of multiple genes in gastric carcinoma: association with histological type and CpG island methylator phenotype. *Cancer Sci* 2003; 94: 901-5.
34. Toyooka S, Toyooka KO, Harada K, Miyajima K, Makarla P, Sathyanarayana UG, Yin J, Sato F, Shivapurkar N, Meltzer SJ, Gazdar AF. Aberrant methylation of the CDH13 (H-cadherin) promoter region in colorectal cancers and adenomas. *Cancer Res* 2002; 62: 3382-6.
35. Song SH, Jong HS, Choi HH, Kang SH, Ryu MH, Kim NK, Kim WH, Bang YJ. Methylation of specific CpG sites in the promoter region could significantly down-regulate p16(INK4a) expression in gastric adenocarcinoma. *Int J Cancer* 2000; 87: 236-40.
36. Kang GH, Lee S, Shim YH, Kim JC, Ro JY. Profile of methylated CpG sites of hMLH1 promoter in primary gastric carcinoma with microsatellite instability. *Pathol Int* 2002; 52: 764-8.
37. Sarbia M, Geddert H, Klump B, Kiel S, Iskender E, Gabbert HE. Hypermethylation of tumor suppressor genes (p16INK4A, p14ARF and APC) in adenocarcinomas of the upper gastrointestinal tract. *Int J Cancer* 2004; 111: 224-8.
38. Lee TL, Leung WK, Chan MW, Ng EK, Tong JH, Lo KW, Chung SC, Sung JJ, To KF. Detection of gene promoter hypermethylation in the tumor and serum of patients with gastric carcinoma. *Clin Cancer Res* 2002; 8: 1761-6.
39. Waki T, Tamura G, Tsuchiya T, Sato K, Nishizuka S, Motoyama T. Promoter methylation status of E-cadherin, hMLH1, and p16 genes in nonneoplastic gastric epithelia. *Am J Pathol* 2002; 161: 399-403.